Turkish Journal of Physics
http://journals.tubitak.gov.tr/physics/
Research Article

Turk J Phys
(2015) 39: 199 – 207

doi:10.3906/fiz-1502-4

A full relativistic treatment in analyzing α-^{12}C and α-^{40,42,44,48}Ca elastic scattering data at 1.37 GeV

Zuhair Fayyad Mahmoud SHEHADEH*
Physics Department, Taif University, Taif, Saudi Arabia

Received: 06.02.2015 • **Accepted/Published Online:** 25.05.2015 • **Printed:** 30.07.2015

Abstract: A simple optical potential of Woods–Saxon form is used within the framework of the Klein–Gordon equation, for the first time, to analyze the elastic differential cross sections for 1.37 GeV (lab) incident α-particles on ^{12}C and calcium isotopes ^{40,42,44,48}Ca. The relativistic energy–momentum relation assures the need for relativistic calculations. As such, the previously determined parameters of all optical potential forms, used in the nonrelativistic Schrödinger equation and successfully analyzing the α-^{12}C and α-^{40,42,44,48}Ca data at 1.37 GeV, are to be revised. In the presence of Coulomb potential, as in the cases under consideration, the asymptotic solution of the Klein–Gordon equation differs from the corresponding one for the Schrödinger equation and the codes are modified accordingly.

Key words: Alpha-nucleus potential, elastic scattering, high energy physics

PACS No. 25.80.Dj, 11.80.-m, 24.10.Ht

1. Introduction

The high-energy scattering of alpha particles from different nuclei has been of considerable importance for studying interesting phenomena and gleaning important information about nuclear matter distributions [1]. Contrary to protons, alpha particles have neither spin nor isospin. This has given them an advantage to be used as spectroscopic probes for nuclear densities and to unravel certain nuclear mysteries. Although Glauber's nucleus–nucleus scattering theory [2] has been successful in describing high-energy hadron-nucleus elastic scattering data, it is still far from complete. In fact, its success is considered more qualitative than quantitative. This is very clear in its use in the analyses of α-^{12}C and α-^{40,42,44,48}Ca at 1.37 GeV. The "rigid projectile" assumption [3,4] leads to a better description, but not a complete one, for the interaction of alpha particles with ^{40}Ca at 1.37 GeV. Moreover, the impulse approximation, using either a simple nucleon–alpha interaction or the nucleon–alpha t-matrix models, only gives a fair agreement to the α-^{12}C experimental elastic differential cross sections at small angles ($\theta < 10°$) for the 1.37 GeV incident α-particles [5]. Nevertheless, Antonov et al. [6] have tried to analyze the experimental data of elastic alpha-particle, with 1.37 GeV incident kinetic energy, scattering on ^{12}C and ^{40,42,44,48}Ca in the framework of the model of coherent fluctuations of nuclear density, called the coherent fluctuations model. Although their analyses are remarkably successful compared to all previous ones, they still underestimate the second and third minima for α-^{12}C and the third minima for α-^{40,42,44,48}Ca cases

In astrophysics, it is well known that alpha particles represent more than 10% of the primary galactic

*Correspondence: zfs07@hotmail.com

cosmic ray flux [7]. This warrants a study on the nuclear interactions of high-energy alpha particles with spacecraft. The collision of space elements, from hydrogen to nickel, with the walls of spacecraft usually causes a serious hazard of radiation to astronauts as well as instruments, mainly microelectronic measuring devices, in the cabin [8]. Sabra et al. [9] have studied the fragmentation of silicon by alpha-particles at incident energies up to 1.0 GeV (cm). Such a study required knowledge of the potential between two emerging fragments, which is taken to be an optical potential of molecular type [10].

The complexity and limited success of all the mentioned theoretical models and theories have led interested researchers to use an optical potential of Woods–Saxon form, used in the nonrelativistic Schrödinger equation, to describe available high-energy alpha-nucleus elastic scattering data. In fact, Bauhoff [11] and Nakano et al. [12] have reported different results about the nature of the real part of an optical potential. Another study [13] has suggested that the optical potential should be weakly attractive to account for the observed minima in the α-^{12}C and α-^{40,42,44,48}Ca elastic differential cross sections. Furthermore Khoa et al. [14] have suggested different optical potential forms, used in the nonrelativistic Schrödinger equation with relativistic kinematics [15], to reanalyze the alpha-calcium data at 1.37 GeV. Although all these studies suggested and used an optical model to explain the elastic differential cross sections for the α-^{12}C and α-^{40,42,44,48}Ca at 1.37 GeV, they unfortunately met with limited success. In addition, the high energy double-folding optical potential with the first and second order corrections to the eikonal phase shifts [16] did not do any better. In their paper, Bonin et al. [17] measured alpha-nucleus elastic differential cross sections, and tried analyzing them using optical potentials with Woods–Saxon forms.

Recently, Shehadeh [18–20] has used different optical potential forms to analyze pion-nucleus elastic scattering data using the Klein–Gordon equation. Adopting a complete relativistic treatment, the agreements between theory and experiment, in analyzing $\pi^{\pm}-$nucleus elastic scattering data, were very satisfactory. This creates a strong inducement to use an optical potential in the Klein–Gordon equation, instead of the nonrelativistic Schrödinger equation, to describe α-^{12}C and α-^{40,42,44,48}Ca elastic scattering data at 1.37 GeV. This is evidently justified since one can show that, by simply using the relativistic energy–momentum equation [21], the scattering of alpha particles at such high energy is relativistic.

As such, we are going to investigate here the use of a Woods–Saxon optical potential form, for both real and imaginary parts, in the full Klein–Gordon equation to explain the α-^{12}C and α-^{40,42,44,48}Ca measured elastic differential cross sections at 1.37 GeV, and to settle the debate about the nature of the potential. Section 2 presents the theory. Section 3 is concerned with the results and discussion. It includes new potential parameters that are different from any previously reported ones. The major conclusions of this investigation are summarized in section 4.

2. Theory

The use of an optical potential, within the framework of the nonrelativistic Schrödinger equation with only relativistic kinematics to substitute for all relativistic effects, proves to be unsuccessful in explaining the data reasonably well. As such, we investigate here the use of an optical potential, with Woods–Saxon form for both its real and imaginary parts, within the framework of the full Klein–Gordon equation. The radial part of the Klein–Gordon equation has the following form [22]:

$$\frac{d^2\chi_{n,\ell}(r)}{dr^2} + \left[k^2 - \frac{2E}{\hbar^2 c^2}\left(V(r) - \frac{V^2(r)}{2E}\right) - \frac{\ell(\ell+1)}{r^2}\right]\chi_{n,\ell}(r) = 0, \tag{1}$$

with

$$k^2 = \frac{E^2 - \mu^2 c^4}{\hbar^2 c^2}, \tag{2}$$

where $\hbar, c$, μ, and E are, respectively, Planck's constant divided by 2π, velocity of light in a vacuum, reduced mass, and total energy of the two colliding particles; and $V(r)$ is the sum of the complex nuclear part $V_N(r)$ and the Coulomb potential $V_C(r)$, i.e. $V(r) = V_N(r) + V_C(r)$. The Coulomb potential $V_C(r)$ is considered due to a uniformly charged spherical distribution given by

$$V_C(r) = \begin{cases} \frac{Z_p Z_T e^2}{8\pi\varepsilon_o R_C}\left(3 - \frac{r^2}{R_C^2}\right) & r \le R_C \\ \frac{Z_p Z_T e^2}{4\pi\varepsilon_o r} & r > R_C \end{cases} \tag{3}$$

where Z_p, Z_T, e, ε_o, and R_C are, respectively, the projectile atomic number, target atomic number, electronic charge, permittivity of free space, and Coulomb radius.

Outside the nuclear radius, $V_N(r) = 0$ compared to the Coulomb and centrifugal terms, Eq. (1) reduces to

$$\frac{d^2\chi_{n,\ell}(r)}{dr^2} + \left[k^2 - \frac{2E}{\hbar^2 c^2}V(r) - \frac{\beta - \ell(\ell+1)}{r^2}\right]\chi_{n,\ell}(r) = 0, \tag{4}$$

with

$$\beta = \frac{V_C^2(r)}{(\hbar^2 c^2)\, r^2} = \frac{Z_p^2 Z_T^2 e^4}{(4\pi)^2 \varepsilon_o^2 \hbar^2 c^2} = \frac{Z_p^2 Z_T^2}{(4\pi)^2 \varepsilon_o^2}\alpha^2, \tag{5}$$

where $\alpha = e^2/\hbar c \cong 1/137$ is the Sommerfeld fine-structure constant.

The solution of Eq. (4) in terms of the dimensionless variable $\rho = kr$ is expressed as

$$\chi_{n,\ell}(\rho) \underset{r\to\infty}{\longrightarrow} \sqrt{A_\ell^2(k) + B_\ell^2(k)} * \left\{ \begin{array}{l} \sin\left[\rho - \eta\ln(2\rho) - \frac{\pi}{2}\left(\gamma + \frac{1}{2}\right) + \arg\Gamma\left(\gamma + i\eta + \frac{1}{2}\right)\right] \\ + (-1)^\ell \tan\delta_\ell \cos\left[\rho - \eta\ln(2\rho) - \frac{\pi}{2}\left(\gamma + \frac{1}{2}\right) + \arg\Gamma\left(\gamma + i\eta + \frac{1}{2}\right)\right] \end{array} \right\} \tag{6}$$

where $A_\ell(k) = X_\ell(k)\sin\delta_\ell$ and $B_\ell(k) = X_\ell(k)\cos\delta_\ell$ are the coefficients of the linear combination with δ_ℓ being the phase shift for the partial wave ℓ. Here η and γ are defined as

$$\eta = \frac{Z_p Z_T e^2 E}{4\pi\varepsilon_o k}, \tag{7}$$

$$\gamma = \sqrt{\left(\ell + \frac{1}{2}\right)^2 - \frac{Z_p Z_T e^2}{(4\pi\varepsilon_o)^2}}, \tag{8}$$

i.e. γ is not an integer, and the recursion relations used for the nonrelativistic Schrödinger equation do not hold any more. Therefore, the calculations are done for each ℓ, which is, no doubt, a lengthy and tedious process.

It is worth noting that when the squared potential term, $V^2(r)/2E$, in the Klein–Gordon equation is neglected, Eq. (1) reduces to the nonrelativistic Schrödinger equation with all well-known subsequent dues.

The argument of the gamma function is evaluated by using the following series expansion [23]:

$$\arg\Gamma(x + iy) = y\psi(x) + \sum_{n=0}^{\infty}\left[\frac{y}{x+n} + \tan^{-1}\left(\frac{y}{x+n}\right)\right] \tag{9}$$

with

$$\psi\left(x\right)=\frac{\Gamma'\left(x\right)}{\Gamma\left(x\right)}=\frac{d}{dx}\left[\ln\Gamma\left(x\right)\right] \tag{10}$$

and

$$\ln\Gamma\left(x\right)\cong\left(x-\frac{1}{2}\right)\ln x-\frac{1}{2}\ln\left(2\pi\right)+\frac{1}{12x}-\frac{1}{360x^3}+\frac{1}{1260x^5}+... \tag{11}$$

Usually the experimental values are in the laboratory system, while the theoretical ones are in the center of mass system. As such, one needs to find the kinetic energy of the projectile in the center of mass system (T_{cm}) from the kinetic energy in the laboratory system (T_L), and the appropriate relation is [24]

$$T_{cm}=-\left(m_p+m_T\right)c^2+\sqrt{\left(m_T-m_p\right)^2c^4+2m_Tc^2T_L}, \tag{12}$$

where m_p and m_T are the projectile and target rest masses.

The nuclear potential adopted in this investigation has the following form:

$$V\left(r\right)=Vf\left(x_v\right)+iWf\left(x_w\right)+V_C\left(r\right), \tag{13}$$

with $f\left(x\right)=\left(1+e^x\right)^{-1}$, $x_i=\left(r-R_i\right)/a_i$, and $V_C\left(r\right)$ as given in Eq. (3).

To obtain the phase shifts δ_ℓ for each ℓ, the logarithmic derivative of the inner solution, evaluated by using Numerov's integration method, is matched with the outer one of the asymptotic solution. For a complete relativistic treatment, we have used here the relativistic Coulomb functions instead of the nonrelativistic ones. As such, one can calculate the scattering amplitude $f\left(\theta\right)$ given by

$$f\left(\theta\right)=\frac{1}{2ik}\sum_{\ell=0}^{\infty}i^\ell\left(2\ell+1\right)\left\{1-e^{2i\left[\arg\Gamma\left(\gamma+i\eta+\frac{1}{2}\right)-\eta\ln(2\rho)-\frac{\pi}{2}\left(\gamma+\frac{1}{2}\right)+\delta_\ell\right]}\right\}P_\ell\left(\cos\theta\right). \tag{14}$$

The elastic scattering differential cross section, $d\sigma/d\Omega$, is defined as

$$\frac{d\sigma}{d\Omega}=\left|f\left(\theta\right)\right|^2, \tag{15}$$

and the reaction cross section, σ_r, has the form

$$\sigma_r=\frac{\pi}{k^2}\sum_{\ell=0}^{\infty}\left(2\ell+1\right)\left[1-\left|S_\ell\right|^2\right] \tag{16}$$

where the complex scattering matrix S_ℓ is related to the scattering phase shifts δ_ℓ by $S_\ell=e^{2i\delta_\ell}$.

3. Results and discussion

Many theories, theoretical models, and approximations have treated the scattering of 1.37 GeV α particles from ^{12}C and ^{40,42,44,38}Ca nonrelativistically. In addition, all previous optical potential forms that tried to explain the measured elastic differential cross sections at 1370 MeV incident energy for α-^{12}C and α-^{40,42,44,48}Ca systems are used within the framework of the nonrelativistic Schrödinger equation. Yet no reasonable physical agreement has been achieved between theory and experiment for these systems. On the other hand, the relativistic energy–momentum relation reveals the need for relativistic treatment for the nuclear cases under consideration. In fact, the speed (v) of a 1370 MeV incident alpha-particle is about 0.7 the speed of light in a vacuum (c); i.e. v $\approx$ 0.7c, which is relativistic. As such, we have treated the scattering cases under consideration as completely relativistic.

In this regard, the parameters of our potentials are listed in the Table. These parameters are totally different from any previously reported parameters, which assures that our potentials are new updated ones. The calculated elastic differential cross sections, compared to the measured ones, along with the potentials used, are shown in Figures 1–3.

Table. The potential parameters V (in MeV), R_v (in fm), a_v (in fm), W (in MeV), R_w (in fm), and a_w (in fm), used in Eq. (13) for α-particles with energy $T_\alpha = 1370$ incident on carbon-12 and calcium isotopes. Our calculated reaction cross sections σ_r in millibarns and volume integrals, real J_R and imaginary J_I, in MeV.fm^3 are noted in columns 8, 9, and 10, respectively.

Target	V	R_v	a_v	W	R_w	a_w	σ_r	J_R	J_I
^{12}C	–39.0	2.60	0.44	–135.0	1.97	0.75	471.7	–62.6	–294.6
^{40}Ca	–62.0	3.68	0.53	–77.0	3.80	0.85	1085.2	–97.4	–165.2
^{42}Ca	–45.0	3.85	0.57	–77.0	3.80	0.85	1085.9	–77.8	–165.2
^{44}Ca	–41.0	3.98	0.57	–77.0	3.80	0.85	1086.8	–73.9	–150.2
^{48}Ca	–35.0	4.28	0.44	–77.0	3.98	0.85	1158.6	–66.1	–137.7

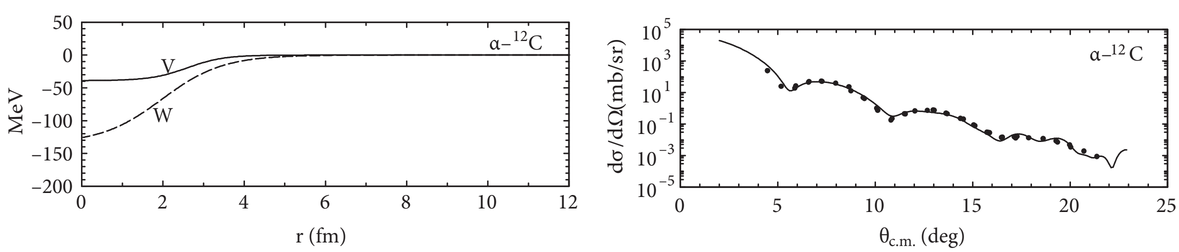

Figure 1. In the right part, the calculated angular distributions (solid line) are compared with the observed angular distributions [9] (solid circles) for the scattered alpha particles from ^{12}C at 1370 MeV. These angular distributions are obtained by using the real and imaginary parts of the potential, V and W, respectively, for the parameters listed in the Table, represented by solid and dashed lines in the left part of the figure.

In Figure 1, the agreement between theory and experiment is excellent over all the angular range and not only at smaller angles [5]. Our calculated reaction cross section is also in excellent agreement with the values reported by Peng et al. [25] and Khoa et al. [14]. This is a remarkable success for our optical potential, used within the framework of the Klein–Gordon equation, compared to all other theoretical models. While Antonov et al. [6] have attributed the unsuccessful description of the α-^{12}C scattering to some peculiarities of the ^{12}C structure, Viollier and Turtschi [3] have interpreted the noticeable discrepancy between theory and experiment as being due to anomalies in the target nucleus ^{12}C. Moreover, the approach, based on the multiple diffraction scattering theory and α-cluster model [17], did not explain the measured elastic differential cross sections for α-^{12}C interaction at 1370 MeV.

Although there have been improvements in analyzing α-^{40,42,44,48}Ca data, deficiencies still exist. As an example, the potential parameters of the optical potentials reported in the literature [12,14] changed randomly

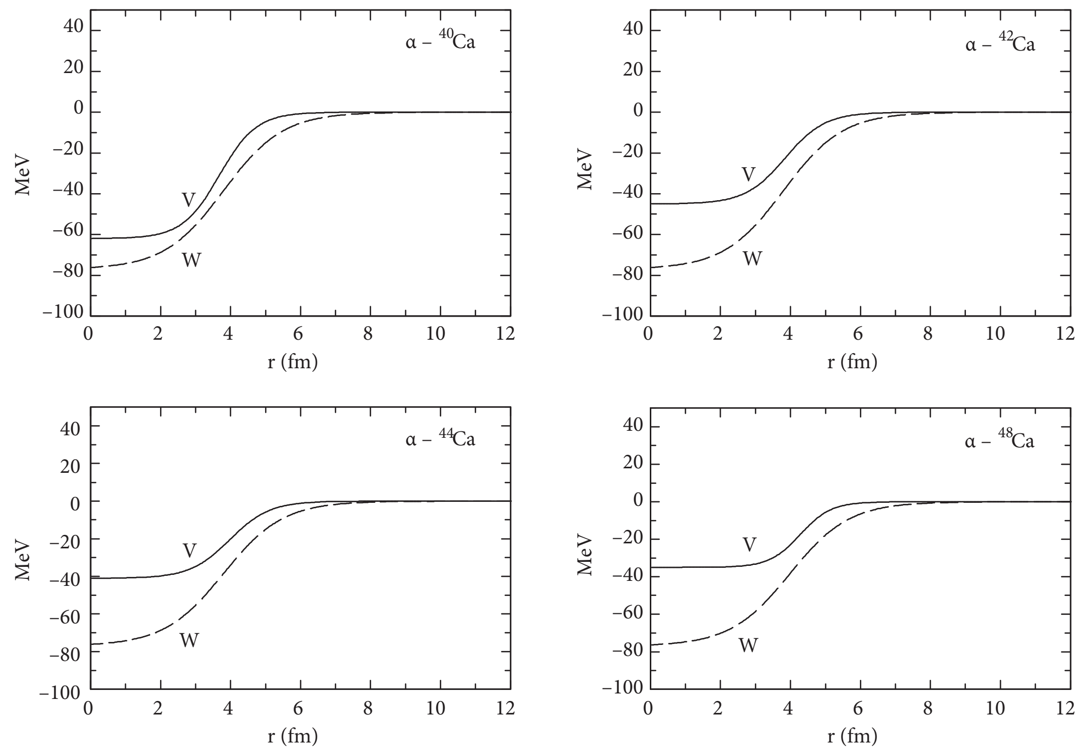

Figure 2. The real and imaginary parts of the potential, V and W, respectively, for the parameters listed in the Table and used in the analyses of α-^{40,42,44,48}Ca scattering data at $T_\alpha = 1370$ MeV.

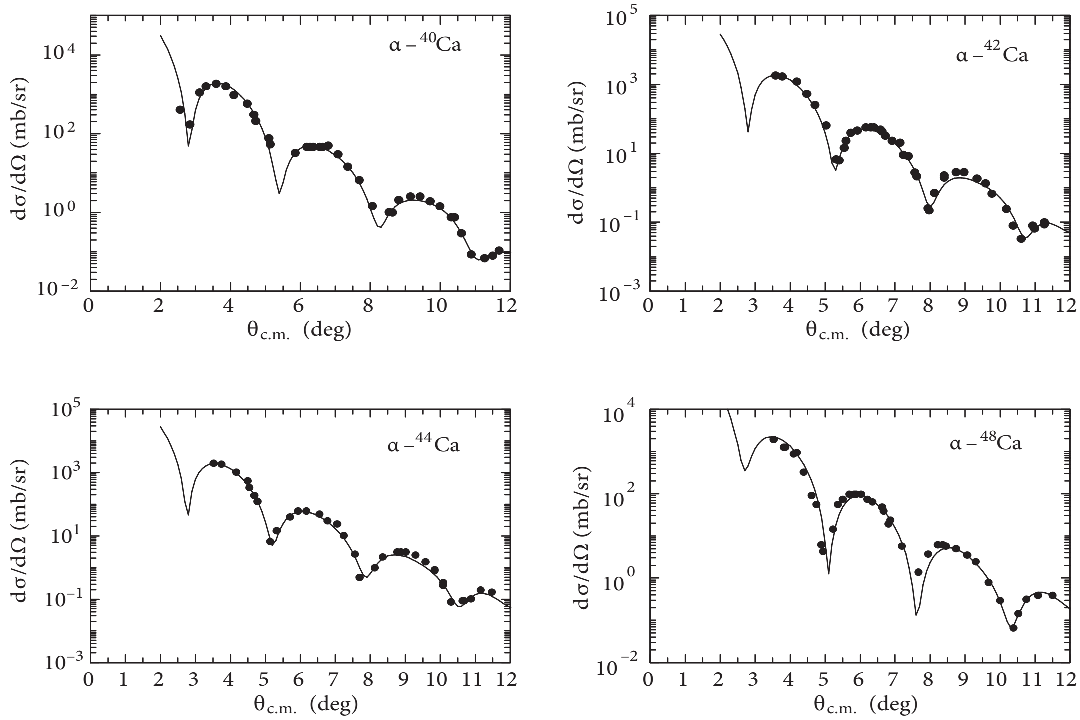

Figure 3. The calculated angular distributions (solid lines) are compared with the observed angular distributions [9] (solid circles) for the scattered alpha particles from ^{40,42,44,48}Ca . These angular distributions are obtained by using the potential forms, represented in Figure 2, in the Klein–Gordon equation.

and did not follow a certain trend. Moreover, maxima and minima that appear in the experimental elastic differential cross sections were not well accounted for [3]. Undoubtedly, these maxima and minima are crucial in fixing the potential parameters and in determining correctly the nature of the potential. The rectification of these deficiencies was always kept in mind in this investigation. Obviously our potential parameters listed in the Table, namely the depth V and the radius R_v of the real part of the potential, show a decrease and a systematic increase, respectively, with the mass number of the target nucleus. It is worth mentioning that the increase in R_v did not follow the $A^{1/3}$ rule (A is the atomic mass of the target nucleus) as in the similar nonrelativistic treatments. In fact, this is dominant in the relativistic treatments. A careful look at the Table reveals that V, for calcium isotopes, decreases with increasing mass number, while the parameters of the imaginary part are kept unchanged except for a slight increase in R_w for ^{48}Ca isotope. The decrease in V might indicate that the three calcium isotopes, ^{42,44,48}Ca, are more compact than ^{40}Ca. One can also note that the trend in the decrease of V is in accord with the values reported by Nakano et al. [12], and related to the neutron excess in the ^{42,44,48}Ca isotopes. In fact, our V-values are the same as Nakano et al.'s ones, for ^{42,44,48}Ca, multiplied by a factor of 6.3. It has been noted that the depth of the real part, V, is crucial in accounting for the angular distributions, especially the dips, as presented in Figure 4. This point was also stressed by Nakano et al. [12]. Furthermore, for ^{48}Ca in particular, one may note an abrupt decrease in the real diffuseness parameter, a_v, which may be attributed to a small neutron skin for this doubly closed shell isotope [26] and, as such, to nuclear matter distribution [27]. With our obtained potential parameters, the calculated reaction cross sections for α-^{40}Ca are in good agreement with the values reported by Khoa et al. [14]. On the other hand, our calculated reaction cross sections are in good agreement with the ones reported by Nakano et al. [12], especially for α-^{42}Ca, using the Mexican-hat shape potential. In their work, they assumed that σ_r is due to the surface interaction and approximated by

$$\sigma_r(A_1) = \left(\frac{A_1}{A_2}\right)^{2/3} \sigma_r(A_2), \tag{17}$$

where A_1 and A_2 are the mass numbers of two nuclei.

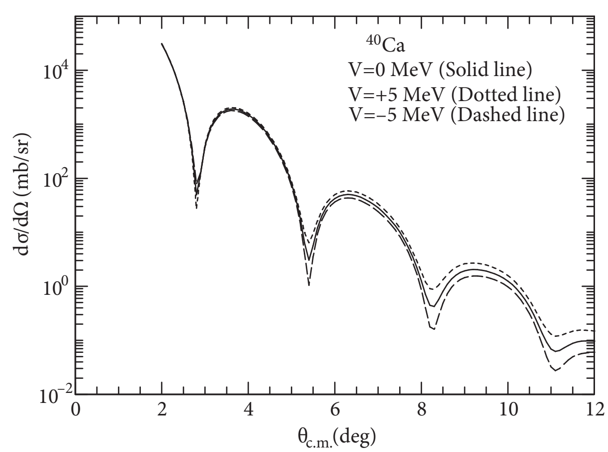

Figure 4. The calculated angular distributions for various V-values while the other five parameters are kept unchanged. The solid line shows the best-fit angular distributions with V = –62 MeV. The dashed and dotted lines show the angular distributions with V = –5 MeV and V= +5 MeV, respectively.

In fact, the reported values for the reaction cross sections using both Woods–Saxon and Mexican-hat potential shapes differ in magnitude and trend.

Our successful results achieved by complete relativistic treatment for alpha-nucleus scattering at 1.37 GeV, implementing our potential in the Klein–Gordon equation, settle the debate about the nature of alpha-nucleus potential at the indicated energy. Both parts, real and imaginary, of our optical potential are attractive as shown in Figures 1 and 2. It is interesting to point out that the approximated relation in (17) applies nicely for our calculated cross sections. Obviously if one considers $\sigma_r(A_1) = 471.7\,mb$ for ^{12}C, the values of the obtained $\sigma_r(A_2)$ for calcium isotopes are in nice agreement with the ones listed in the Table.

In the Table, the calculated real and imaginary volume integrals per nucleon, J_R and J_I, respectively, given by

$$J_R = \frac{4\pi}{A_P A_T}\int_0^\infty V(r)\, r^2 dr, \tag{18}$$

and

$$J_I = \frac{4\pi}{A_P A_T}\int_0^\infty W(r)\, r^2 dr, \tag{19}$$

where A_P and A_T are the mass numbers of projectile and target nuclei, are listed.

The values for J_R and J_I are in accord with the published ones $J_R \approx -70\,MeV.fm^3$ and $J_I \approx -170\,MeV.fm^3$ for the optical potential used in the analysis of p-^{40}Ca elastic scattering experiments [28]. The negative values of J_R and J_I reflect the negative potential strengths for the real and imaginary parts of our adopted potential. In addition, the noticeable decrease in J_R for the three calcium isotopes, ^{42,44,48}Ca, compared to J_R for ^{40}Ca is in accord with the corresponding decrease in V. One needs to emphasize here that all these good simultaneous results are obtained in connection with the forward-angle available data. For a uniquely determined potential and strong confidence of such a potential, large-angle elastic scattering data are needed.

4. Conclusions

This investigation indicates the necessity for using a nuclear optical potential of Woods–Saxon form, within a relativistic framework, to describe correctly high-energy alpha-nucleus scattering data. The Klein–Gordon equation, rather than the Schrödinger equation, is the correct one for the relativistic description of α-nucleus interaction at $T_\alpha = 1370\,MeV$. As such, our potential parameters are totally new and different from any other published ones. In fact, the attractive nature of both parts of the potential is demonstrated. With such a potential, the α-^{12}C and α-^{40,42,44,48}Ca experimental elastic differential cross sections are nicely accounted for, and our calculated reaction cross sections and volume integrals are strong supporters of the adopted potential. Based on the available forward-angle data, the obtained simultaneous good results are a trademark of promising potential. This potential may contribute positively to nuclear astrophysics and nuclear technology.

Acknowledgments

The author acknowledges the financial support of the Deanship of Scientific Research at Taif University, Taif, Saudi Arabia, for this investigation. This paper is dedicated to the soul of Prof FB Malik, who passed away while this work was in its intermediate stages.

References

[1] Viollier, R D. In *XVII International Winter Meeting on Nuclear Physics*, Bormio, Italy, 1979, p. 1.

[2] Glauber, J. *Lectures in Theoretical Physics* **1959**, *1*, 315–414.

[3] Viollier, R. D.; Turtschi, E. *Ann. Phys.* **1980,** *124*, 290–312.

[4] Alkhazov, G. D.; Bauer, T.; Bertini, R.; Bimbot, L.; Bing, O.; Boudard, A.; Bruge, G.; Catz, H.; Chaumeaux, A.; Couvert, P.; et al. *Nucl. Phys. A* **1977**, *280*, 365–376.

[5] Chaumeaux, A.; Bruge, G.; Bauer, T.; Bertini, R.; Boudard, A.; Catz, H.; Couvert, P.; Duhm, H. H.; Fontaine, J. M.; Garreta, D.; et al. *Nucl. Phys. A* **1976**, *267*, 413–424.

[6] Antonov, A. N.; Nikolaev, V. A.; Petkov, I. Zh. *Bulg. J. Phys.* **1983**, *10*, 42–49.

[7] Cucinotta, F. A.; Townsend, L. W.; Wilson, J. W. *NASA Technical Paper No. 3285*, 1993.

[8] Wilson, J. W.; Townsend, L. W.; Schimmerling, W.; Khandelwal, G. S.; Khan, F.; Nealy, J. E.; Cucinotta, F. A.; Simonsen, L. C.; Shinn, J. L.; Norbury, J. W. *NASA Reference Publication No. 1257*, 1991.

[9] Sabra, M. S.; Shehadeh, Z. F.; Malik, F. B. *Eur. Phys. J. A* **2006**, *27*, 167–181.

[10] Shehadeh, Z. F.; Basak, A. K.; Abdullah, M. N. A.; Uddin, M. A.; Reichstein, I.; Sabra, M. S.; Malik, F. B. *Int. J. Mod. Phys. B* **2007**, *21*, 2429–2437.

[11] Bauhoff, W. *Z. Phys. A* **1986**, *323*, 219–222.

[12] Nakano, M.; Matsuura, H.; Maki, T.; Matoba, M.; Ohgaki, H. *Phys. Rev. C* **1989**, *40*, 1323–1334.

[13] Satchler, G. R. In *Proceedings of the International Nuclear Physics Conference*, Bristol, England, 1987, p.397.

[14] Khoa, D. T.; Satchler, G. R.; Thuy, N. D. *Phys. Rev. C* **2002**, *65*, 024611-10.

[15] Farid, M. E.; Satchler, G. R. *Phys. Lett. B* **1984**, *146*, 389–391.

[16] Hassan, M. Y. H.; Metawei, Z. *Acta Physica Slovaca* **2002**, *52*, 23–34.

[17] Bonin, B.; Alamanos, N.; Bruge, G.; Faraggi, H; Lugol, J. C.; Mittig, W.; Papineau, L.; Yavin, A. I.; Arvieux, J.; Farvacque, L.; et al. *Nucl. Phys. A* **1985**, *445*, 381–407.

[18] Shehadeh, Z. F. *Int. J. Mod. Phys. E* **2009**, *18*, 1615–1627.

[19] Shehadeh, Z. F. *Turk. J. Phys.* **2013**, *37*, 190–197.

[20] Shehadeh, Z. F. *J. Mod. Phys.* **2014**, *5*, 341–352.

[21] Shehadeh, Z. F.; Alam, M. M.; Malik, F. B. *Phys. Rev. C* **1999**, *59*, 826–831.

[22] Shehadeh, Z. F.; Scott, J. S.; Malik, F. B. *AIP Conf. Proc.* **2011**, *1370*, 185–191.

[23] Abramowitz, M.; Stegun, I. A. *Handbook of Mathematical Functions*; Dover: New York, NY, USA, 1972.

[24] Eder, G. *Nuclear Forces: Introduction to Theoretical Nuclear Physics*; Massachusetts Institute of Technology Press: Boston, MA, USA, 1968.

[25] Peng, J. C.; Devries, R. M.; Digiacomo, N. J. *Phys. Lett. B* **1981**, *98*, 244–247.

[26] Gils, H. J.; Friedman, E.; Rebel, H.; Buschmann, J.; Zagromski, S.; Klewe-Nebenius, H.; Neumann, B.; Pesl, R.; Bechtold, G. *Phys. Rev. C* **1980**, *21*, 1239–1244.

[27] Streets, J.; Brown, B. A.; Hodgson, P. E. *J. Phys. G: Nucl. Phys.* **1982**, *8*, 839–850.

[28] Arnold, L. G.; Clark, B. C.; Cooper, E. D.; Sherif, H. S.; Hutcheon, D. A.; Kitching, P.; Cameron, J. M.; Liljestrand, R. P.; McDonald, W. J.; Miller, C. A.; et al. *Phys. Rev. C* **1982**, *25*, 936–940.